

DR JI YU (Orcid ID : 0000-0001-6868-1218)

PROFESSOR XINYONG LIU (Orcid ID : 0000-0002-5833-3807)

Article type : Research Article

Design, Synthesis and Evaluation of Novel Heteroaryldihydropyrimidines Derivatives as Non-nucleoside Hepatitis B Virus Inhibitors by Exploring the Solvent-exposed Region

Ji Yu,[†] Xiaowei Guo,[/] Samuel Desta,[†] Shuo Zhang,[†] Jian Zhang,[†] Xiao Ding,[†] Xiaohong
Liang,^{*,/} Haiyong Jia,^{*,§} Xinyong Liu^{*,†} and Peng Zhan^{*,†}

[†] Department of Medicinal Chemistry, Key Laboratory of Chemical Biology (Ministry of Education), School of Pharmaceutical Sciences, Shandong University, 44 West Culture Road, 250012 Jinan, Shandong, PR China

[/] Department of Immunology, Key Laboratory for Experimental, Teratology of Ministry of Education, Shandong Provincial Key Laboratory of Infection and Immunology, Shandong University School of Medicine, Jinan 250012, Shandong Province, PR China

[§] School of Pharmacy, Weifang Medical University, 261053 Weifang, Shandong, PR China

AUTHOR INFORMATION

Corresponding Authors

*Xiaohong, Liang.: e-mail, liangxiaohong@sdu.edu.cn.

*Haiyong, Jia.: e-mail, 502378774@163.com; phone, 15063389092.

*Xinyong, Liu.: e-mail, xinyongl@sdu.edu.cn; phone, 086-531-88380270.

*Peng, Zhan.: e-mail, zhanpeng1982@sdu.edu.cn; phone, 086-531-88382005

This article has been accepted for publication and undergone full peer review but has not been through the copyediting, typesetting, pagination and proofreading process, which may lead to differences between this version and the Version of Record. Please cite this article as doi: 10.1111/cbdd.13512

This article is protected by copyright. All rights reserved.

ABSTRACT

In continuation of our efforts toward the discovery of potent non-nucleoside HBV inhibitors with novel structures, we have explored the solvent-exposed protein region of heteroaryldihydropyrimidines (HAPs) derivatives. Herein, the morpholine ring of GLS4 was replaced with substituted sulfonamides and triazoles to generate novel non-nucleoside HBV inhibitors with desirable potency. In *in vitro* biological evaluation, several derivatives showed good anti-HBV DNA replication activity compared to lamivudine. In particular, compound **II-1** displayed the most potent activity against HBV DNA replication ($IC_{50} = 0.35 \pm 0.04 \mu M$). The preliminary structure-activity relationships (SARs) of the new compounds were summarized, which may help in discovering more potent anti-HBV agents via rational drug design.

KEYWORDS: HBV, capsid, HAP, sulfonamide, triazoles, protein-solvent interface

INTRODUCTION

Chronic hepatitis B (CHB), a global therapeutic problem caused by the hepatitis B virus (HBV), infects over 250 million people worldwide especially in Asia-Pacific regions. About one third of these individuals develop life-threatening diseases such as liver failure, cirrhosis and hepatocellular carcinoma (HCC) with over 650,000 deaths every year.¹ Currently therapies are limited to the use of interferons (interferon-alpha and pegylated interferon) and nucleoside/nucleotide reverse transcriptase inhibitors (NRTIs): lamivudine (3TC), entecavir (ETV), telbivudine (LdT), adefovir dipivoxil (ADV), tenofovir disoproxil (TDF) and tenofovir alafenamide (TAF) (**Figure 1**).² Both therapies can reduce HBV DNA and normalize liver enzymes. However, they can't eradicate chronic HBV infection, as viral covalently closed circular DNA (cccDNA) yet remains.³ Furthermore, interferons are poorly tolerated and expensive, and the usage of NRTIs results in long-term treatment and drug-resistance.⁴ As none of these inhibitors can cure HBV infections, there is always an urgent need to develop more effective and safety drugs with novel chemical structures and mechanisms of action.

(Figure 1)

HBV capsid protein plays essential roles in key steps of HBV life cycle such as reverse transcription of pregenomic RNA (pgRNA), formation and intracellular trafficking of relaxed circular DNA and subviral particle formation, which has been a novel drug target in recent years.⁵ Currently, great progress have been made in the development of HBV capsid inhibitors (or effectors), as exemplified by several drug candidates, including DVR-23, AT-130, Bay 41-4109 and GLS4 (Figure 2).⁶

(Figure 2)

Heteroaryldihydropyrimidines (HAPs) were identified as novel HBV capsid assembly inhibitors, which can prevent the normal assembly of core protein and lead to a formation of misassembled capsid.^{7,8} What's more, the misassembled capsid was then degraded by host proteasomes.⁹ In 2001, Bayer company firstly reported Bay 41-4109 ($IC_{50} = 124.25$ nM), a potential HAP compound that prevent HBV infections by reducing HBV viral DNA in the liver and plasma. However, it was found out to be hepatotoxic at high doses ($CC_{50} = 35$ μ M). After years of structural optimization based on bioisosterism and computer-aided drug design, GLS4 ($IC_{50} = 62.24$ nM, $CC_{50} = 115$ μ M), with improved activity and decreased toxicity was discovered and is currently in the phase II clinical stage. In addition, GLS4 also had potent anti-HBV activity against adefovir-resistant strains with IC_{50} of 12 nM.^{10,11}

Even so, the poor water solubility and oral bioavailability of GLS4 limited the chance of being developed into a market drug, therefore, in the past several years, systematic structural modifications have performed on this core structure.^{9,12} In this article, we have tried to employ rational drug design strategies to explore the chemically diverse space of GLS4, with the aim to enhance anti-HBV activity and improve water solubility and in vitro safety profiles. To obtain some enlightenment, detailed SARs of existing HAPs were summarized as follows:

1-position of HAPs: the hydrogen of pyrimidine is necessary for the activity as substituted alkyl groups are not favored at this position. Interestingly, the fused ring analogs could moderate to excellent potency; **2-position of HAPs:** high-polarity rings significantly reduce activity, thiazolyl is the most suitable substituent at this position; **4-position of HAPs:** phenyls bearing fluorine, chlorine and bromine are well tolerated while polar and bulky

groups are not favored; **5-position of HAPs:** polar and large groups are not favored, methyl or ethyl ester appear to be the most favorable groups; **6-position of HAPs:** polar and hydrophilic groups (such as carboxyl) at this position are favored. They could significantly reduce liposolubility of the compounds, and form hydrogen bond with critical residues nearby the protein-solvent interface such as Ser121 and Ser141.^{12,13}

(Figure 3)

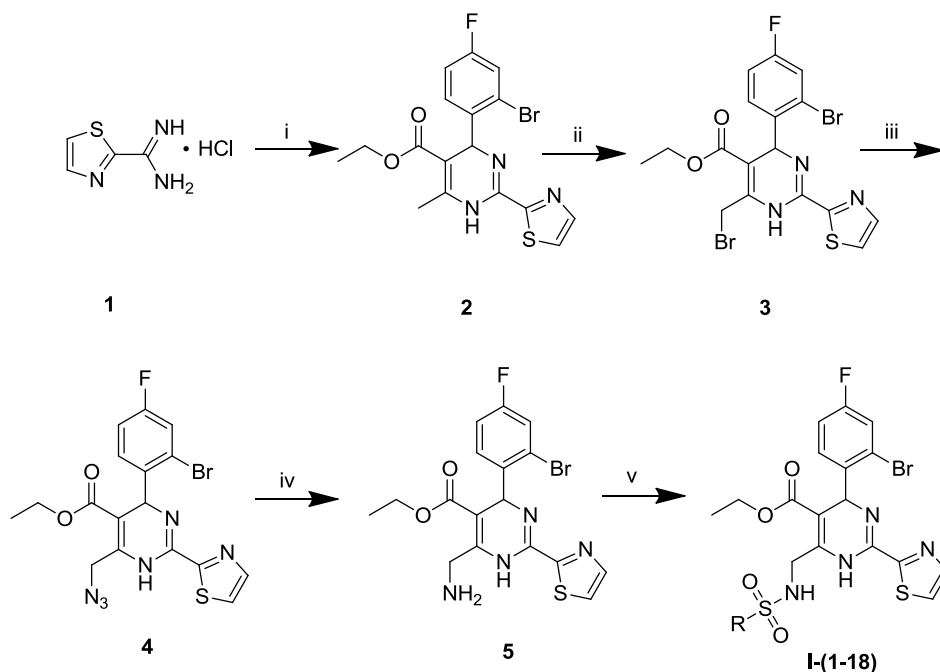
Sulfonamide groups possess several unique physicochemical properties. They are able to modulate solubility and acid-base property and improve binding affinity through hydrogen bond interactions, that are extensively used in drug design.^{14,15} Besides, with the development of structural biology, we have investigated some X-ray crystal structures of HBV core protein in complex with 4-methyl HAPs (PDB ID: 5GMZ) and sulfamoylbenzamides (PDB ID: 5T2P), discovering sulfonamide may be well tolerated at the solvent-exposed region, as it overlaps pretty well with the carboxyl pharmacophore (**Figure 3**).¹² Meanwhile, considering the poor *in vivo* instability of GLS4, we replaced the morpholine ring with substituted triazoles to improve the metabolic stability and anti-HBV activity. Herein, we report the design, synthesis and *in vitro* biological evaluation of novel anti-HBV HAP-sulfonamide and HAP-triazole derivatives (**Figure 4**).

(Figure 4)

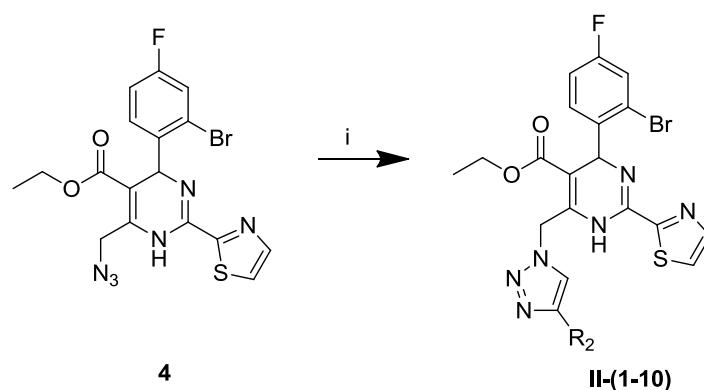
CHEMISTRY

The synthetic routes of HAP derivatives **I-(1-18)** and **II-(1-10)** were illustrated in **Scheme 1** and **2**. The key intermediate **2**, prepared from the commercially available 2-thiazolecarboxamidine hydrochloride (**1**), 2-bromo-4-fluorobenzaldehyde and ethyl acetoacetate by classic “Biginelli reaction” was converted to intermediate **3** with NBS and CCl₄ by free radical reaction. Using acetone as solvent, the intermediate **3** was reacted with NaN₃ to give intermediate **4** by nucleophilic substitution reaction,¹⁶ which was further reduced to intermediate **5** via one-step “Staudinger reaction”.¹⁷ Finally, target compounds **I-(1-18)** were obtained from intermediate **5** by easy condensation reaction with DCM, Et₃N

and different substituted sulfonyl chloride as raw materials (**Scheme 1**), and target compounds **II-(1-10)** were obtained from intermediate **4** by CuAAC reaction (**Scheme 2**).



Scheme 1. Reagents and Conditions: (i) 2-bromo-4-fluorobenzaldehyde, ethyl acetoacetate, CH_3COONa , EtOH, 80 °C; (ii) NBS, CCl_4 , 50 °C; (iii) NaN_3 , acetone, r.t.; (iv) PPh_3 , THF, H_2O , r.t.; (v) for **I-(1-3)** and **I-(5-18)**: substituted sulfonyl chloride, Et_3N , DCM, r.t.; for **I-4**: cyclopropanesulfonyl chloride, Et_3N , DMF, 90 °C.



Scheme 2. Reagents and Conditions: (i) $\text{CuSO}_4 \cdot 5\text{H}_2\text{O}$, Sodium ascorbate, H_2O , THF, r.t.

RESULTS AND DISCUSSION

The target compounds were evaluated for their cytotoxicity, inhibitory effect on HBV DNA replication and HBsAg and HBeAg secretion in HepG2.2.15 cells (human HBV transgenic hepatocellular carcinoma cells) via cell counting kit-8 (CCK-8), PCR and standard ELISA method, respectively. The biological results were represented as inhibition percentages, IC₅₀ values, CC₅₀ values and selectivity index (SI) values (determined as the CC₅₀/IC₅₀ values).^{18,19}

The cytotoxicity of HAP-sulfonamide derivatives **I-(1~18)** were measured by cell counting kit-8 (CCK-8) method in HepG2.2.15 cell line. As shown in **Table 1**, most of these analogues exhibited low toxicity under the concentration of 20 μ M (Inhibition percentages < 50%). It was shown that phenyl group bearing one or more methyl improved the toxicity of the inhibitors; for instance, **I-8**, **I-9**, **I-10** and **I-17** with the inhibition percentages of $43.1 \pm 3.3\%$, $45.1 \pm 2.7\%$, $43.3 \pm 0.9\%$ and $45.2 \pm 6.2\%$, respectively. When the substituent had short aliphatic chain (methyl, ethyl or propyl), the corresponding inhibitors showed no toxicity at the tested concentration (**I-1**, **I-2** and **I-3**).

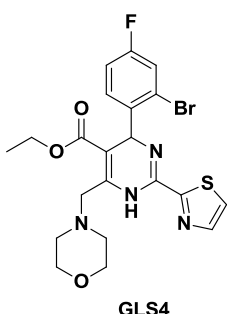
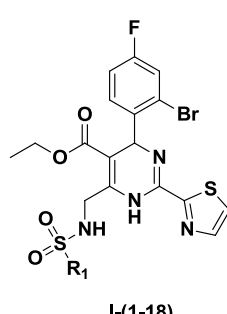

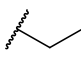
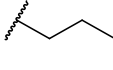
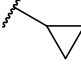
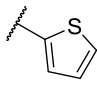
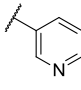
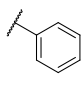
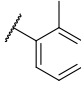
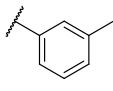
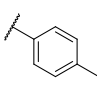
The cytotoxicity of HAP-triazole derivatives were also illustrated in **Table 2**. We identified that substitution of large group at R₂ improved the toxicity of the inhibitors (**II-8**: $97.8 \pm 0.2\%$; **II-9**: $73.2 \pm 3.8\%$). Phenyl substitution of R₂ made no contribution to the toxicity (**II-5**) while phenyl group bearing -NH₂ exhibited high toxicity, especially -NH₂ on *meta*- and *para*- positions (**II-2** and **II-6**).

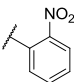
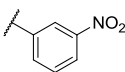
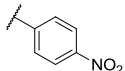
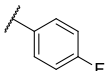
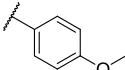
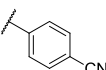
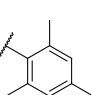
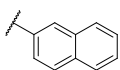
The inhibitory effects on HBV DNA replication of HAP-sulfonamide derivatives were screened in the HepG2.2.15 cell line using GLS4 and 3TC as the positive controls. In the first-round screen, following the treatment of cells with the tested compounds at 20 μ M for 8 days, the extracellular HBV DNA were collected and then quantified by real-time FQ-PCR. As shown in **Table 1**, some of HAP-sulfonamide derivatives such as **I-5**, **I-11**, **I-13**, **I-15** and **I-17** showed better inhibitory activities ($72.6 \pm 1.3\%$, $80.6 \pm 0.7\%$, $80.1 \pm 4.2\%$, $78.4 \pm 0.6\%$ and $76.7 \pm 8.0\%$, respectively) against HBV DNA replication compared to 3TC ($72.3 \pm 15.0\%$). Primary SARs were summarized as follows:

First, we introduced a short aliphatic chain at R₁ position, and obtained activity in the following sequence: propyl > methyl > ethyl (**I-3** > **I-1** > **I-2**). Next, R₁ replacement by heterocycles indicated the order of anti-HBV DNA replication activity as follows: thiophene > benzene > naphthalene > pyridine (**I-5** > **I-7** > **I-18** > **I-6**). In addition, SAR of the substituent group at benzene ring was studied. The results suggested that strong electron-withdrawing group (NO₂) appeared to be the most favorable group (**I-11** and **I-13**), closely followed by other substituents in the following sequence: OCH₃ > CH₃ > F > CN (**I-15** > **I-8** > **I-14** > **I-16**). More specifically, the substitution pattern in the benzene ring played an essential role in maintaining anti-HBV activity. *Ortho*- and *para*- substituents were favored and showed similar activity (**I-8** vs **I-10**, **I-11** vs **I-13**) whereas *meta*-position counterparts (**I-9** and **I-12**) dropped the activity.

The inhibitory effects on HBV DNA replication of HAP-triazole derivatives (20 μM) were illustrated in **Table 2**. To investigate the effects of different aromatic substituents in the position of R₂, six derivatives **II-(1-6)** were synthesized and assessed for anti-HBV activity. Compared to **II-3** (73.1 ± 3.3%) and **II-4** (76.5 ± 8.3%), compound **II-5** (81.9 ± 5.9%) showed better activity, which suggested that phenyl was superior to pyridine and thiophene. However, **II-5** lost its activity when the concentration dropped to 5 μM (-0.7%). Furthermore, *Ortho*- substituent was found to be more preferable than *meta*- and *para*- substituents (**II-1** > **II-2** > **II-6**). In addition, large substituents on position R₂ was studied (**II-(8-10)**). Compound **II-9** showed anti-HBV activity (82.0 ± 4.4%) but also had high cytotoxicity (73.2 ± 3.8%).

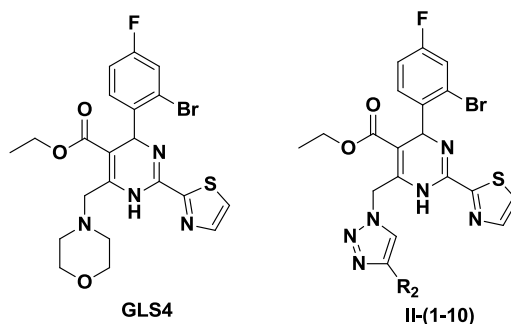
Table 1. Anti-HBV activity, cytotoxicity of HAP-sulfonamide derivatives **I-(1~18)** and positive drug GLS4 and 3TC.^a

 <p>GLS4</p>		 <p>I-(1-18)</p>	
Compounds	R ₁	Inhibition percentages (%)	
		DNA	HepG2.2.15 Cell
I-1		21.2 ± 15.5	-13.4 ± 14.4
I-2		0.4 ± 1.4	33.9 ± 1.1
I-3		66.5 ± 5.2	14.9 ± 14.3
I-4		23.9 ± 5.9	20.9 ± 8.5
I-5		72.6 ± 1.3	43.9 ± 3.4
I-6		19.5 ± 4.3	22.7 ± 7.8
I-7		61.8 ± 2.9	36.7 ± 11.9
I-8		65.3 ± 2.8	43.1 ± 3.3
I-9		57.1 ± 7.2	45.1 ± 2.7
I-10		67.0 ± 3.7	43.3 ± 0.9

I-11		80.6 ± 0.7	-35.6 ± 0.3
I-12		69.8 ± 3.7	28.8 ± 8.0
I-13		80.1 ± 4.2	43.9 ± 4.9
I-14		60.5 ± 7.0	17.3 ± 17.5
I-15		78.4 ± 0.6	25.3 ± 14.3
I-16		19.6 ± 15.9	13.7 ± 9.1
I-17		76.7 ± 8.0	45.2 ± 6.2
I-18		47.8 ± 5.7	14.8 ± 12.7
GLS4		94.6 ± 0.04	-0.5 ± 0.01
3TC		72.3 ± 15.0	3.7 ± 5.7

^a HepG2.2.15 cells were cultured in the presence of HAP-sulfonamide derivatives, GLS4 and 3TC at 20 μM for 8 days, and then extracellular HBV DNA levels were quantified by real-time FQ-PCR, cytotoxicity were quantified by CCK-8.

Table 2. Anti-HBV activity, cytotoxicity of HAP-triazole derivatives **II-(1~10)** and positive drug GLS4 and 3TC.^a



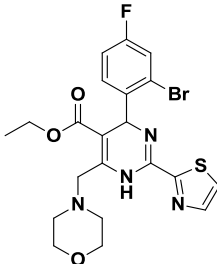
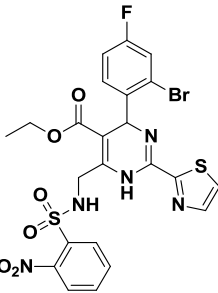
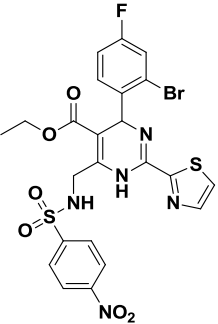
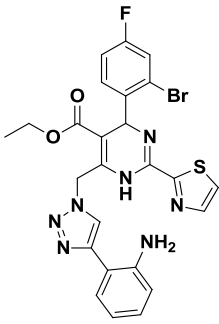
Compounds	R ₂	Inhibition percentages (%)	
		DNA	HepG2.2.15 Cell
II-1		86.2 ± 4.8	12.2 ± 16.8
II-2		78.7 ± 2.5	60.7 ± 4.4
II-3		73.1 ± 3.3	66.5 ± 4.5
II-4		76.5 ± 8.3	14.4 ± 11.0
II-5		81.9 ± 5.9	8.4 ± 12.1
II-5 (5 μM)		-0.7	6.3 ± 5.8
II-6		75.9 ± 4.8	59.1 ± 5.6
II-7		78.9 ± 4.8	1.7 ± 7.3
II-8		ND ^b	97.8 ± 0.2
II-9		82.0 ± 4.4	73.2 ± 3.8
II-10		9.6 ± 0.5	41.3 ± 11.4
GLS4		91.8 ± 0.8	38.2 ± 22.7
3TC		74.9 ± 4.7	-2.3 ± 1.6

^a HepG2.2.15 cells were cultured in the presence of HAP-triazole derivatives, GLS4 and 3TC at 20 μM for 8 days, and then extracellular HBV DNA levels were quantified by real-time FQ-PCR, cytotoxicity were quantified by CCK-8.

^b ND: not determined.

The activity of compound **I-11**, **I-13** and **II-1** were further evaluated in HepG2.2.15 cells in a dose-dependent manner (50 μ M, 5 μ M, 0.5 μ M, 0.05 μ M, 0.005 μ M) to analyze their IC_{50} and CC_{50} values. Among them, **II-1** showed the best in vitro anti-HBV DNA activity ($IC_{50} = 0.35 \pm 0.04 \mu$ M), which was 1.8-fold higher than that of 3TC ($IC_{50} = 0.62 \pm 0.31 \mu$ M). The potency of **I-13** ($IC_{50} = 0.76 \pm 0.12 \mu$ M) was close to 3TC, being 4.5-fold higher than **I-11** ($IC_{50} = 3.52 \pm 0.64 \mu$ M) (Table 3). All these three compounds had no cytotoxicity in the tested concentration ($CC_{50} > 50 \mu$ M).

Table 3. Anti-HBV DNA replication activity, cytotoxicity and selectivity indices of HAP derivatives (**I-11**, **I-13** and **II-1**) and positive drug GLS4 and 3TC.

			
GLS4	I-11	I-13	II-1
Compounds	CC_{50}^a (μ mol/L)	DNA	
		IC_{50}^b (μ mol/L)	SI ^c
I-11	> 50	3.52 ± 0.64	> 14.2
I-13	> 50	0.76 ± 0.12	> 65.8
II-1	> 50	0.35 ± 0.04	> 143
GLS4	> 50	0.051 ± 0.001	> 980.4
3TC	> 50	0.62 ± 0.31	> 80.6

^a IC_{50} : Concentrations of compounds achieving 50% inhibition of DNA replication.

^b CC_{50} : Concentrations of compounds required to reduce the viability of HepG2.2.15 cells by 50%.

^c SI: selectivity index, the ratio of CC_{50}/IC_{50} .

Compound **II-1** was further evaluated for its inhibitory effect on HBsAg and HBeAg secretion in HepG2.2.15 cells in a dose-dependent manner (50 μ M, 5 μ M, 0.5 μ M, 0.05 μ M, 0.005 μ M). However, as illustrated in **Table 4**, **II-1** doesn't have anti-HBsAg and HBeAg secretion activity ($IC_{50} > 50$ μ M). Since GLS4 only had moderate inhibitory values ($IC_{50} = 14.8 \pm 0.75$ and 6.1 ± 0.07 μ M, respectively), we presumed that HAPs don't act directly on antigen secretion.

Table 4. Anti-HBsAg and HBeAg secretion activity, cytotoxicity and selectivity indices of **II-1** and positive drug GLS4 and 3TC.

Compounds	HBsAg		HBeAg	
	IC_{50}^a (μ mol/L)	SI ^b	IC_{50} (μ mol/L)	SI
II-1	> 50	—	> 50	—
GLS4	14.8 ± 0.75	1.5	6.1 ± 0.07	3.7
3TC	> 100	—	> 100	—

^a IC_{50} : Concentrations of compounds achieving 50% inhibition of DNA replication.

^b SI: selectivity index, the ratio of CC_{50}/IC_{50} .

MOLECULAR MODELING STUDIES

II-1, the best compound in cell-based HBV infection assay, was docked into the HBV capsid (PDB ID: 5e0i) using Sybyl-X 2.0 to study its binding mode. Default parameters were used as described in the Sybyl-X 2.0 manual unless otherwise specified, and the result was displayed by PyMOL.

(Figure 5)

As is shown in **Figure 5**, the results indicated that the Br, F-substituted phenyl region occupied a hydrophobic pocket, surrounded by Pro25, Asp29, Leu30, Thr33, Trp102 and Ile105 (chain B). The 2-thiazolyl group interacted with Phe23 (chain B) and Thr128 (chain C), being coplanar with the dihydropyrimidine core as previously reported.¹² Interestingly, the designed triazole fragment nearby the protein-solvent interface interacted with some crucial

residues, which might contribute to the anti-HBV activity. Two N atoms of triazole ring can form a hydrogen bond with Thr128 (chain C). Besides, the “-NH₂” of phenyl ring also interacted with Ser121 (chain C) by hydrogen bonding. In addition, the benzene ring was likely to interact with Pro134 (chain C) by Van der Waals' force.

PHYSICOCHEMICAL PROPERTIES PREDICTION

Furthermore, some physicochemical properties of the **II-1** were calculated using free online software (<http://www.molinspiration.com/>). As shown in **Table 5**, active compounds **II-1** conformed well to the Lipinski's rule of five, which could be considered as a promising lead compound for further development.

Table 5. Prediction of physicochemical properties^a of **II-1**.

Compd.	nViol	MW	Natoms	miLogP	nON	nOHNH	Nrotb	TPSA	MV
II-1	1	582.46	37	3.40	9	3	8	120.33	443.18

^anViol: no. of violations; natoms: no. of atoms; miLogP: molinspiration predicted LogP; MW: molecular weight; nON: no. of hydrogen bond acceptors; nOHNH: no. of hydrogen bond donors; nrotb: no. of rotatable bonds; TPSA: topological polar surface area; MV: molar volume.

CONCLUSION

In conclusion, novel HAP-sulfonamide and HAP-triazole derivatives were designed and synthesized as non-nucleoside anti-HBV inhibitors. All the designed compounds were evaluated for their bioactivities against HBV DNA replication. Among them, compound **II-1** was found to be the most potent, with IC₅₀ value of 0.35 ± 0.04 μM, which was 1.8-fold higher than 3TC (IC₅₀ = 0.62 ± 0.31 μM). The anti-HBeAg and HBsAg secretion activity (IC₅₀ > 50 μM) of **II-1** indicated that it doesn't act directly on antigen secretion. Furthermore, molecular modeling study carried out to predict the interactions between **II-1** and HBV capsid suggested that the H-bond interaction formed by “-NH₂” of phenyl ring and Ser121

was important in the binding of this compound. The results of some physicochemical properties of **II-1** like miLogP measured showed **II-1** conformed well to the Lipinski's rule of five. The preliminary SARs of the new compounds were summarized, which may help discovering more potent anti-HBV agents with diverse structures.

EXPERIMENTAL SECTION

Chemistry. All melting points were measured with a micromelting point apparatus and are uncorrected. ^1H NMR and ^{13}C NMR spectra were performed on a Bruker AV-400 spectrometer (Bruker BioSpin, Switzerland) or Bruker AV-300 spectrometer (Bruker BioSpin, Switzerland) using tetramethylsilane (TMS) as internal reference and DMSO- d_6 or CDCl_3 as solvent. Chemical shifts were expressed in δ units (ppm) and J values were presented in hertz (Hz). Mass spectra were taken on a LC Autosampler Device: Standard G1313 instrument. TLC was performed on Silica Gel GF254 for TLC (Merck) and spots were visualized by irradiation with UV light (254 nm). Flash column chromatography was performed on column packed with Silica Gel 60 (200-300 mesh). Solvents were reagent grade and, when necessary, were purified and dried by standard methods. Rotary evaporators served in concentration of the reaction solutions at reduced pressure.

General procedure for the synthesis of intermediate 2. To the mixture solution of 2-thiazolecarboxamidine hydrochloride (0.50 g, 3.05 mmol) in ethanol (50 mL), 2-bromo-4-fluorobenzaldehyde (0.93 g, 4.60 mmol) and ethyl acetoacetate (600 μL , 4.60 mmol) were added. The resulting mixture was stirred for 6 h at 80 $^\circ\text{C}$. The reaction mixture was cooled and the solvent was evaporated under reduced pressure. The residue was taken up with water (60 mL) and extracted with EtOAc (25 mL \times 3), and the organic phase was washed with saturated sodium chloride (25 mL), dried over anhydrous Na_2SO_4 , evaporated under reduced pressure to give the corresponding crude product. The residue was dissolved in a small amount EtOAc and purified by column chromatography on silica gel using PE-EA system to give intermediate **2** in good yield.

Ethyl

4-(2-bromo-4-fluorophenyl)-6-methyl-2-(thiazol-2-yl)-1,4-dihydropyrimidine-5-carboxylate

(2). Yellow solid, yield 58%, mp: 158–160 °C; ¹H NMR (400 MHz, CDCl₃) δ 7.81 (d, J = 2.8 Hz, 1H), 7.46 (s, 1H), 7.38–7.28 (m, 2H), 6.97 (t, J = 8.2 Hz, 1H), 6.15 (s, 1H), 4.05 (q, J = 7.1 Hz, 2H), 2.53 (s, 3H), 1.13 (t, J = 7.1 Hz, 3H); EI-MS: 424.3 [M+H]⁺.

General procedure for the synthesis of intermediate 3. To the mixture solution of intermediate 2 (0.50 g, 1.17 mmol) in CCl₄ (50 mL), NBS (0.22 g, 1.24 mmol) were added slowly. The resulting mixture was stirred for 2 h at 50 °C. The reaction mixture was cooled and the solvent was evaporated under reduced pressure. The residue was added with water (60 mL) and extrated with EtOAc (25 mL × 3), and the organic phase was washed with saturated sodium chloride (25 mL), dried over anhydrous Na₂SO₄, evaporated under reduced pressure to give the corresponding crude product. The residue was dissolved in a small amount EtOAc and purified by column chromatography on silica gel using PE-EA system to give intermediate 3 in good yield.

Ethyl

4-(2-bromo-4-fluorophenyl)-6-(bromomethyl)-2-(thiazol-2-yl)-1,4-dihydropyrimidine-5-carboxylate (3).

Yellow solid, yield 59%, mp: 125–127 °C; ¹H NMR (400 MHz, CDCl₃) δ 7.84 (d, J = 3.1 Hz, 1H), 7.52 (s, 2H), 7.44–7.35 (m, 1H), 7.32 (dd, J = 8.1, 2.6 Hz, 1H), 7.02 (t, J = 8.0 Hz, 1H), 6.09 (s, 1H), 4.94 (d, J = 8.9 Hz, 1H), 4.61 (s, 1H), 4.09 (d, J = 7.0 Hz, 2H), 1.16 (t, J = 7.1 Hz, 3H); EI-MS: 502.2 [M+H]⁺.

General procedure for the synthesis of intermediate 4. To the mixture solution of intermediate 3 (0.50 g, 1.00 mmol) in acetone (45 mL) were added with NaN₃ (0.13 g, 2.00 mmol). The resulting mixture was stirred overnight at room temperature. The solvent was evaporated under reduced pressure. The residue was taken up with water (60 mL) and extrated with EtOAc (25 mL × 3), and the organic phase was washed with saturated sodium chloride (25 mL), dried over anhydrous Na₂SO₄, evaporated under reduced pressure to give the corresponding crude product. The residue was dissolved in a small amount EtOAc and choromatographed on silica gel using PE-EA system to give intermediate 4 in good yield.

Ethyl

6-(azidomethyl)-4-(2-bromo-4-fluorophenyl)-2-(thiazol-2-yl)-1,4-dihydropyrimidine-5-carboxylate (**4**). Yellow solid, yield 80%, mp: 126–128 °C; ¹H NMR (400 MHz, CDCl₃) δ 8.64 (s, 1H), 7.85 (d, *J* = 3.1 Hz, 1H), 7.55 (d, *J* = 3.1 Hz, 1H), 7.48–7.37 (m, 1H), 7.35–7.29 (m, 1H), 7.10–6.92 (m, 1H), 6.29–6.02 (m, 1H), 4.97 (s, 1H), 4.60 (d, *J* = 2.6 Hz, 1H), 4.17–4.00 (m, 2H), 1.13 (t, *J* = 7.1 Hz, 3H); ¹³C NMR (100 MHz, CDCl₃) δ 165.78, 165.03, 163.31, 162.71, 162.36, 162.09, 160.80, 160.22, 154.83, 150.00, 143.92, 143.54, 143.10, 142.75, 139.59, 137.74 (d, *J* = 3.5 Hz), 130.80, 130.72, 130.61, 124.92, 123.38, 122.07 (d, *J* = 9.7 Hz), 120.23 (dd, *J* = 24.4, 17.0 Hz), 115.83, 115.62, 115.18, 114.97, 106.27, 98.60, 77.37, 77.06, 76.74, 60.70, 60.32, 58.37, 51.91 (d, *J* = 2.0 Hz), 49.79, 14.07 (d, *J* = 5.7 Hz); EI-MS: 465.4 [M+H]⁺.

General procedure for the synthesis of intermediate 5. To the mixture solution of THF (30 mL) and H₂O (10 mL) were added with intermediate **4** (0.37 g, 0.80 mmol) and PPh₃ (0.21 g, 0.80 mmol). The resulting mixture was stirred for 4 h at 35 °C. Upon completion of the reaction, the mixture was taken up with water (60 mL) and extracted with EtOAc (25 mL × 3), and the organic phase was washed with saturated sodium chloride (25 mL), dried over anhydrous Na₂SO₄, evaporated under reduced pressure to give the corresponding crude product. The residue was dissolved in a small amount EtOAc and purified by column chromatography, using PE-EA as eluent to give intermediate **5** in good yield.

Ethyl

6-(aminomethyl)-4-(2-bromo-4-fluorophenyl)-2-(thiazol-2-yl)-1,4-dihydropyrimidine-5-carboxylate (**5**). Yellow solid, yield 37%; ¹H NMR (400 MHz, DMSO) δ 7.99 (t, *J* = 5.5 Hz, 1H), 7.93 (d, *J* = 3.1 Hz, 1H), 7.55 (dd, *J* = 8.6, 2.6 Hz, 1H), 7.37 (dd, *J* = 8.6, 6.3 Hz, 1H), 7.21 (td, *J* = 8.5, 2.6 Hz, 1H), 5.98 (d, *J* = 11.9 Hz, 1H), 4.76 (d, *J* = 89.1 Hz, 3H), 4.00 (d, *J* = 13.5 Hz, 2H), 3.94 (q, *J* = 7.0 Hz, 2H), 1.05 (t, *J* = 7.1 Hz, 3H); EI-MS: 439.4 [M+H]⁺.

General procedure for the synthesis of target compounds I-(1-3) and I-(5-18). To the mixture solution of intermediate **5** (0.10 g, 0.23 mmol) in DCM (10 mL) were added with substituted sulfonyl chloride (0.46 mmol) and Et₃N (60 μL, 0.46 mmol). The resulting mixture was stirred for 5 h at room temperature. Upon completion of the reaction, the mixture was added to water (50 mL) and extracted with EtOAc (20 mL × 3), and the organic phase was

washed with saturated sodium chloride (25 mL), dried over anhydrous Na₂SO₄, evaporated under reduced pressure to give the corresponding crude product. The residue was dissolved in a small amount EtOAc and purified by column chromatography using PE-EA as eluent. Crystallization of this material from DCM-Hexane gave the target compounds **I-(1~3)** and **I-(5~18)** in good yield.

Ethyl

4-(2-bromo-4-fluorophenyl)-6-(methylsulfonamidomethyl)-2-(thiazol-2-yl)-1,4-dihydropyrimidine-5-carboxylate (I-1). Yellow solid, yield 59%, mp: 132–134 °C; ¹H NMR (400 MHz, DMSO) δ 9.35 (s, 1H), 8.01 (d, *J* = 3.1 Hz, 1H), 7.95 (d, *J* = 3.0 Hz, 1H), 7.71 (s, 1H), 7.58 (dd, *J* = 8.6, 2.4 Hz, 1H), 7.44 (dd, *J* = 8.6, 6.3 Hz, 1H), 7.23 (td, *J* = 8.5, 2.5 Hz, 1H), 6.02 (s, 1H), 4.56 (d, *J* = 4.1 Hz, 2H), 3.97 (q, *J* = 7.0 Hz, 2H), 3.05 (s, 3H), 1.05 (t, *J* = 7.1 Hz, 3H); EI-MS: 517.5 [M+H]⁺; HRMS *m/z* C₁₈H₁₈BrFN₄O₄S₂: calcd 515.9937, found 517.0009 [M+H]⁺.

Ethyl

4-(2-bromo-4-fluorophenyl)-6-(ethylsulfonamidomethyl)-2-(thiazol-2-yl)-1,4-dihydropyrimidine-5-carboxylate (I-2). Yellow solid, yield 57%, mp: 149–151 °C; ¹H NMR (400 MHz, DMSO) δ 9.35 (s, 1H), 8.01 (d, *J* = 3.1 Hz, 1H), 7.95 (d, *J* = 3.1 Hz, 1H), 7.74 (t, *J* = 6.1 Hz, 1H), 7.58 (dd, *J* = 8.6, 2.4 Hz, 1H), 7.44 (dd, *J* = 8.6, 6.2 Hz, 1H), 7.23 (td, *J* = 8.4, 2.4 Hz, 1H), 6.02 (s, 1H), 4.61–4.48 (m, 2H), 3.97 (q, *J* = 7.0 Hz, 2H), 3.16 (q, *J* = 6.9 Hz, 2H), 1.25 (t, *J* = 7.2 Hz, 3H), 1.05 (t, *J* = 7.1 Hz, 3H); EI-MS: 530.2 [M+H]⁺.

Ethyl

4-(2-bromo-4-fluorophenyl)-6-(propylsulfonamidomethyl)-2-(thiazol-2-yl)-1,4-dihydropyrimidine-5-carboxylate (I-3). Yellow solid, yield 80%, mp: 69–70 °C; ¹H NMR (400 MHz, DMSO) δ 9.37 (s, 1H), 8.02 (d, *J* = 3.0 Hz, 1H), 7.96 (d, *J* = 3.0 Hz, 1H), 7.74 (t, *J* = 6.1 Hz, 1H), 7.58 (dd, *J* = 8.5, 2.3 Hz, 1H), 7.44 (dd, *J* = 8.5, 6.3 Hz, 1H), 7.26–7.20 (m, 1H), 6.02 (s, 1H), 4.56 (qd, *J* = 16.7, 6.2 Hz, 2H), 3.97 (q, *J* = 6.9 Hz, 2H), 3.13 (dt, *J* = 12.1, 6.2 Hz, 2H), 1.71 (dt, *J* = 13.3, 6.7 Hz, 2H), 1.05 (t, *J* = 7.1 Hz, 3H), 0.97 (t, *J* = 7.4 Hz, 3H); EI-MS: 544.2 [M+H]⁺; HRMS *m/z* C₂₀H₂₂BrFN₄O₄S₂: calcd 544.0250, found 545.0323 [M+H]⁺.

Ethyl

4-(2-bromo-4-fluorophenyl)-2-(thiazol-2-yl)-6-((thiophene-2-sulfonamido)methyl)-1,4-dihydropyrimidine-5-carboxylate (**I-5**). Yellow solid, yield 52%, mp: 160–162 °C; ¹H NMR (400 MHz, DMSO) δ 9.20 (s, 1H), 8.55 (s, 1H), 8.03 (d, *J* = 3.1 Hz, 1H), 7.99 (d, *J* = 5.0 Hz, 1H), 7.96 (d, *J* = 3.1 Hz, 1H), 7.68–7.64 (m, 1H), 7.57 (dd, *J* = 8.5, 2.5 Hz, 1H), 7.38 (dd, *J* = 8.6, 6.2 Hz, 1H), 7.23 (dd, *J* = 8.4, 2.2 Hz, 1H), 7.20–7.17 (m, 1H), 5.96 (s, 1H), 4.61 (d, *J* = 16.6 Hz, 1H), 4.47–4.37 (m, 1H), 3.93 (q, *J* = 6.9 Hz, 2H), 1.01 (t, *J* = 7.1 Hz, 3H); EI-MS: 585.1 [M+H]⁺; HRMS *m/z* C₂₁H₁₈BrFN₄O₄S₃: calcd 583.9658, found 584.9730 [M+H]⁺.

Ethyl

4-(2-bromo-4-fluorophenyl)-6-((pyridine-3-sulfonamido)methyl)-2-(thiazol-2-yl)-1,4-dihydropyrimidine-5-carboxylate (**I-6**). Yellow solid, yield 75%, mp: 77–80 °C; ¹H NMR (400 MHz, DMSO-*d*₆) δ 9.30 (s, 1H), 8.98 (d, *J* = 2.4 Hz, 1H), 8.80 (d, *J* = 4.8 Hz, 1H), 8.54 (t, *J* = 6.2 Hz, 1H), 8.19 (t, *J* = 6.6 Hz, 1H), 8.02 (d, *J* = 3.2 Hz, 1H), 7.95 (d, *J* = 3.2 Hz, 1H), 7.58–7.54 (m, 2H), 7.35 (dd, *J* = 8.7, 6.1 Hz, 1H), 7.22–7.18 (m, 1H), 5.90 (s, 1H), 4.64 (dd, *J* = 16.2, 6.4 Hz, 1H), 4.36 (dd, *J* = 16.2, 5.9 Hz, 1H), 3.92 (q, *J* = 6.9 Hz, 2H), 1.00 (t, *J* = 7.0 Hz, 3H); EI-MS: 580.1 [M+H]⁺.

Ethyl

4-(2-bromo-4-fluorophenyl)-6-(phenylsulfonamidomethyl)-2-(thiazol-2-yl)-1,4-dihydropyrimidine-5-carboxylate (**I-7**). Yellow solid, yield 23%, mp: 136–139 °C; ¹H NMR (400 MHz, DMSO) δ 9.20 (s, 1H), 8.35 (t, *J* = 6.2 Hz, 1H), 8.03 (d, *J* = 3.0 Hz, 1H), 7.96 (d, *J* = 3.0 Hz, 1H), 7.83 (d, *J* = 7.4 Hz, 2H), 7.68–7.61 (m, 1H), 7.59–7.53 (m, 3H), 7.35 (dd, *J* = 8.5, 6.3 Hz, 1H), 7.21 (td, *J* = 8.4, 2.4 Hz, 1H), 5.90 (s, 1H), 4.55 (dd, *J* = 16.7, 6.6 Hz, 1H), 4.30 (dd, *J* = 16.8, 5.9 Hz, 1H), 3.91 (q, *J* = 7.1 Hz, 2H), 0.98 (t, *J* = 7.1 Hz, 3H); EI-MS: 579.2 [M+H]⁺.

Ethyl

4-(2-bromo-4-fluorophenyl)-6-((2-methylphenylsulfonamido)methyl)-2-(thiazol-2-yl)-1,4-dihydropyrimidine-5-carboxylate (**I-8**). Yellow solid, yield 37%, mp: 136–138 °C; ¹H NMR (400 MHz, DMSO) δ 9.22 (s, 1H), 8.26 (t, *J* = 6.2 Hz, 1H), 8.03 (d, *J* = 3.1 Hz, 1H), 7.96 (d, *J* = 3.1 Hz, 1H), 7.82 (d, *J* = 7.7 Hz, 1H), 7.58–7.49 (m, 2H), 7.36 (t, *J* = 7.6 Hz, 1H), 7.33–7.26 (m, 2H), 7.20 (td, *J* = 8.4, 2.6 Hz, 1H), 5.82 (s, 1H), 4.66 (dd, *J* = 16.7, 6.7 Hz, 1H), 4.27 (dd,

$J = 16.7, 5.8$ Hz, 1H), 3.91 (q, $J = 7.1$ Hz, 2H), 2.55 (s, 3H), 1.00 (t, $J = 7.1$ Hz, 3H); EI-MS: 593.2 $[M+H]^+$.

Ethyl

4-(2-bromo-4-fluorophenyl)-6-((3-methylphenylsulfonamido)methyl)-2-(thiazol-2-yl)-1,4-dihydropyrimidine-5-carboxylate (**I-9**). Yellow solid, yield 59%, mp: 145–147 °C; ^1H NMR (400 MHz, DMSO) δ 9.17 (s, 1H), 8.28 (t, $J = 6.1$ Hz, 1H), 8.02 (d, $J = 2.9$ Hz, 1H), 7.95 (d, $J = 2.9$ Hz, 1H), 7.60 (d, $J = 12.5$ Hz, 2H), 7.55 (dd, $J = 8.4, 2.1$ Hz, 1H), 7.45–7.38 (m, 2H), 7.33 (dd, $J = 8.3, 6.0$ Hz, 1H), 7.23–7.16 (m, 1H), 5.88 (s, 1H), 4.65 (dd, $J = 16.7, 6.9$ Hz, 1H), 4.25 (dd, $J = 16.7, 5.7$ Hz, 1H), 3.93 (q, $J = 7.1$ Hz, 2H), 2.30 (s, 3H), 1.00 (t, $J = 7.0$ Hz, 3H); EI-MS: 593.2 $[M+H]^+$.

Ethyl

4-(2-bromo-4-fluorophenyl)-6-((4-methylphenylsulfonamido)methyl)-2-(thiazol-2-yl)-1,4-dihydropyrimidine-5-carboxylate (**I-10**). Yellow solid, yield 51%, mp: 78–82 °C; ^1H NMR (400 MHz, DMSO) δ 9.17 (s, 1H), 8.25 (s, 1H), 8.02 (d, $J = 3.1$ Hz, 1H), 7.96 (d, $J = 3.1$ Hz, 1H), 7.69 (d, $J = 8.2$ Hz, 2H), 7.56 (dd, $J = 8.5, 2.4$ Hz, 1H), 7.35 (m, 3H), 7.20 (td, $J = 8.6, 2.5$ Hz, 1H), 5.90 (s, 1H), 4.55 (d, $J = 15.8$ Hz, 1H), 4.26 (d, $J = 16.8$ Hz, 1H), 3.91 (q, $J = 7.1$ Hz, 2H), 2.36 (s, 3H), 0.99 (t, $J = 7.1$ Hz, 3H); EI-MS: 593.2 $[M+H]^+$.

Ethyl

4-(2-bromo-4-fluorophenyl)-6-((2-nitrophenylsulfonamido)methyl)-2-(thiazol-2-yl)-1,4-dihydropyrimidine-5-carboxylate (**I-11**). Yellow solid, yield 70%, mp: 89–92 °C; ^1H NMR (400 MHz, DMSO) δ 9.43 (s, 1H), 8.42 (t, $J = 5.5$ Hz, 1H), 8.05–7.93 (m, 4H), 7.82 (td, $J = 7.5, 1.4$ Hz, 1H), 7.75 (dd, $J = 11.8, 6.8$ Hz, 1H), 7.58–7.53 (m, 1H), 7.31 (dd, $J = 8.6, 6.2$ Hz, 1H), 7.20 (td, $J = 8.6, 2.5$ Hz, 1H), 5.88 (s, 1H), 4.81 (dd, $J = 16.3, 6.0$ Hz, 1H), 4.47 (dd, $J = 16.3, 5.2$ Hz, 1H), 3.93 (q, $J = 7.1$ Hz, 2H), 1.03 (t, $J = 7.1$ Hz, 3H); EI-MS: 624.2 $[M+H]^+$.

Ethyl

4-(2-bromo-4-fluorophenyl)-6-((3-nitrophenylsulfonamido)methyl)-2-(thiazol-2-yl)-1,4-dihydropyrimidine-5-carboxylate (**I-12**). Yellow solid, yield 70%, mp: 163–166 °C; ^1H NMR (400 MHz, DMSO) δ 9.25 (s, 1H), 8.60 (s, 1H), 8.54 (s, 1H), 8.41 (d, $J = 8.2$ Hz, 1H), 8.20 (d, $J = 7.9$ Hz, 1H), 7.96 (d, $J = 3.0$ Hz, 1H), 7.93 (d, $J = 3.0$ Hz, 1H), 7.79 (t, $J = 8.0$ Hz, 1H), 7.54 (dd, $J = 8.4, 2.4$ Hz, 1H), 7.31 (dd, $J = 8.6, 6.2$ Hz, 1H), 7.19 (td, $J = 8.4, 2.9$ Hz, 1H), 5.80 (s,

1H), 4.83 (d, $J = 16.2$ Hz, 1H), 4.29 (d, $J = 16.2$ Hz, 1H), 3.90 (q, $J = 7.1$ Hz, 2H), 1.02 (t, $J = 7.1$ Hz, 3H); EI-MS: 624.2 $[M+H]^+$; HRMS m/z C₂₃H₁₉BrFN₅O₆S₂: calcd 622.9944, found 624.0021 $[M+H]^+$.

Ethyl

4-(2-bromo-4-fluorophenyl)-6-((4-nitrophenylsulfonamido)methyl)-2-(thiazol-2-yl)-1,4-dihydropyrimidine-5-carboxylate (**I-13**). Yellow solid, yield 49%, mp: 98–101 °C; ¹H NMR (400 MHz, DMSO) δ 9.24 (s, 1H), 8.64 (s, 1H), 8.32 (d, $J = 8.7$ Hz, 2H), 8.06 (d, $J = 8.7$ Hz, 2H), 7.99 (d, $J = 3.0$ Hz, 1H), 7.93 (d, $J = 3.1$ Hz, 1H), 7.54 (td, $J = 8.2, 2.3$ Hz, 1H), 7.34 (dd, $J = 8.5, 6.3$ Hz, 1H), 7.20 (dd, $J = 8.2, 6.5$ Hz, 1H), 5.88 (s, 1H), 4.73 (dd, $J = 16.2, 5.0$ Hz, 1H), 4.35 (dd, $J = 16.1, 4.1$ Hz, 1H), 3.94 (q, $J = 7.1$ Hz, 2H), 1.01 (t, $J = 7.0$ Hz, 3H); EI-MS: 624.2 $[M+H]^+$.

Ethyl

4-(2-bromo-4-fluorophenyl)-6-((4-fluorophenylsulfonamido)methyl)-2-(thiazol-2-yl)-1,4-dihydropyrimidine-5-carboxylate (**I-14**). Yellow solid, yield 36%, mp: 82–84 °C; ¹H NMR (400 MHz, DMSO) δ 9.21 (s, 1H), 8.37 (s, 1H), 8.02 (d, $J = 3.0$ Hz, 1H), 7.96 (d, $J = 3.0$ Hz, 1H), 7.89 (dd, $J = 8.2, 5.4$ Hz, 2H), 7.56 (dd, $J = 8.4, 2.2$ Hz, 1H), 7.37 (dt, $J = 10.1, 7.6$ Hz, 3H), 7.24–7.18 (m, 1H), 5.92 (s, 1H), 4.59 (d, $J = 16.1$ Hz, 1H), 4.31 (d, $J = 16.6$ Hz, 1H), 3.93 (q, $J = 7.1$ Hz, 2H), 1.00 (t, $J = 7.0$ Hz, 3H); EI-MS: 597.2 $[M+H]^+$.

Ethyl

4-(2-bromo-4-fluorophenyl)-6-((4-methoxyphenylsulfonamido)methyl)-2-(thiazol-2-yl)-1,4-dihydropyrimidine-5-carboxylate (**I-15**). Yellow solid, yield 57%, mp: 142–144 °C; ¹H NMR (400 MHz, DMSO) δ 9.18 (s, 1H), 8.17 (t, $J = 6.1$ Hz, 1H), 8.02 (d, $J = 3.1$ Hz, 1H), 7.95 (d, $J = 3.1$ Hz, 1H), 7.74 (d, $J = 8.8$ Hz, 2H), 7.56 (dd, $J = 8.6, 2.5$ Hz, 1H), 7.35 (dd, $J = 8.7, 6.2$ Hz, 1H), 7.20 (td, $J = 8.5, 2.5$ Hz, 1H), 7.06 (d, $J = 8.8$ Hz, 2H), 5.91 (s, 1H), 4.54 (dd, $J = 16.8, 6.6$ Hz, 1H), 4.25 (dd, $J = 16.9, 5.7$ Hz, 1H), 3.92 (q, $J = 7.1$ Hz, 2H), 3.82 (s, 3H), 1.00 (t, $J = 7.1$ Hz, 3H); EI-MS: 609.1 $[M+H]^+$.

Ethyl

4-(2-bromo-4-fluorophenyl)-6-((4-cyanophenylsulfonamido)methyl)-2-(thiazol-2-yl)-1,4-dihydropyrimidine-5-carboxylate (**I-16**). Yellow solid, yield 58%, mp: 77–80 °C; ¹H NMR (400 MHz, DMSO) δ 9.22 (s, 1H), 8.58 (s, 1H), 7.99 (m, 5H), 7.89 (d, $J = 8.2$ Hz, 1H), 7.56 (dd, J

= 8.4, 2.5 Hz, 1H), 7.34 (dd, J = 8.5, 6.3 Hz, 1H), 7.21 (td, J = 8.5, 2.4 Hz, 1H), 5.89 (s, 1H), 4.69 (d, J = 16.2 Hz, 1H), 4.34 (d, J = 16.1 Hz, 1H), 3.93 (q, J = 7.1 Hz, 2H), 1.01 (t, J = 7.0 Hz, 3H); EI-MS: 606.1 $[M+H+2]^+$.

Ethyl

4-(2-bromo-4-fluorophenyl)-2-(thiazol-2-yl)-6-((2,4,6-trimethylphenylsulfonamido)methyl)-1,4-dihydropyrimidine-5-carboxylate (**I-17**). Yellow solid, yield 49%, mp: 105–109 °C; ^1H NMR (400 MHz, CDCl_3) δ 7.87 (d, J = 3.0 Hz, 1H), 7.57 (d, J = 3.0 Hz, 1H), 7.45 (s, 1H), 7.30 (dd, J = 8.1, 2.5 Hz, 1H), 7.18 (dd, J = 8.6, 6.0 Hz, 1H), 6.97 (td, J = 8.3, 2.5 Hz, 1H), 6.91 (s, 2H), 6.20 (t, J = 5.5 Hz, 1H), 5.91 (d, J = 1.7 Hz, 1H), 4.38 (qd, J = 16.3, 5.7 Hz, 2H), 4.03 (q, J = 7.1 Hz, 2H), 2.67 (s, 6H), 2.29 (s, 3H), 1.10 (t, J = 7.1 Hz, 3H); EI-MS: 623.4 $[M+H+2]^+$.

Ethyl

4-(2-bromo-4-fluorophenyl)-6-((naphthalene-2-sulfonamido)methyl)-2-(thiazol-2-yl)-1,4-dihydropyrimidine-5-carboxylate (**I-18**). Yellow solid, yield 48%, mp: 145–148 °C; ^1H NMR (400 MHz, DMSO) δ 9.21 (s, 1H), 8.48 (s, 1H), 8.43 (d, J = 6.1 Hz, 1H), 8.12 – 8.01 (m, 3H), 7.99 (d, J = 3.1 Hz, 1H), 7.93 (d, J = 3.0 Hz, 1H), 7.84–7.80 (m, 1H), 7.69 (m, 2H), 7.53 (dd, J = 8.5, 2.4 Hz, 1H), 7.29 (dd, J = 8.5, 6.3 Hz, 1H), 7.12 (td, J = 8.5, 2.2 Hz, 1H), 5.78 (s, 1H), 4.62 (dd, J = 16.7, 6.6 Hz, 1H), 4.33 (dd, J = 16.7, 5.8 Hz, 1H), 3.87 (q, J = 7.1 Hz, 2H), 0.93 (t, J = 7.1 Hz, 3H); EI-MS: 629.2 $[M+H]^+$; HRMS m/z $\text{C}_{27}\text{H}_{22}\text{BrFN}_4\text{O}_4\text{S}_2$: calcd 628.0250, found 629.0324 $[M+H]^+$.

General procedure for the synthesis of target compounds I-4. To the mixture solution of intermediate **5** (0.10 g, 0.23 mmol) in DMF (10 mL) were added with cyclopropanesulfonyl chloride (30 μL , 0.28 mmol) and Et_3N (60 μL , 0.46 mmol). The resulting mixture was stirred for 5 h at 90 °C. Upon completion of the reaction, the mixture was added with water (50 mL) and extracted with EtOAc (20 mL \times 3), and the organic phase was washed with saturated sodium chloride (25 mL), dried over anhydrous Na_2SO_4 , evaporated under reduced pressure to give the corresponding crude product. The residue was dissolved in a small amount EtOAc and purified by column chromatography on silica gel using PE-EA system. Crystallization of this material from DCM-Hexane gave the target compound **I-4** in good yield.

Ethyl

4-(2-bromo-4-fluorophenyl)-6-(cyclopropanesulfonamidomethyl)-2-(thiazol-2-yl)-1,4-dihydropyrimidine-5-carboxylate (**I-4**). Yellow solid, yield 16%, mp: 158–161 °C; ¹H NMR (400 MHz, DMSO) δ 9.29 (s, 1H), 8.01 (d, *J* = 2.8 Hz, 1H), 7.95 (d, *J* = 2.7 Hz, 1H), 7.83 (t, *J* = 5.9 Hz, 1H), 7.57 (d, *J* = 6.5 Hz, 1H), 7.47–7.40 (m, 1H), 7.23 (t, *J* = 8.2 Hz, 1H), 6.02 (s, 1H), 4.63 (ddd, *J* = 22.8, 17.0, 6.3 Hz, 2H), 3.98 (q, *J* = 6.9 Hz, 2H), 2.70 (s, 1H), 1.05 (t, *J* = 7.1 Hz, 3H), 1.01–0.84 (m, 4H); EI-MS: 543.1 [M+H]⁺.

General procedure for the synthesis of lead compounds GLS4. To the mixture solution of intermediate **3** (0.50 g, 1.00 mmol) in DMF (45 mL), morpholine (173 μL, 2.00 mmol) was added. The resulting mixture was stirred overnight at room temperature. The residue was added with water (100 mL) and extrated with EtOAc (25 mL × 3), and the organic phase was washed with saturated sodium chloride (25 mL), dried over anhydrous Na₂SO₄, evaporated under reduced pressure to give the corresponding crude product. The residue was dissolved in a small amount EtOAc and purified by column chromatography on silica gel using PE-EA system to give **GLS4** in good yield.¹⁶

Ethyl

4-(2-bromo-4-fluorophenyl)-6-(morpholinomethyl)-2-(thiazol-2-yl)-1,4-dihydropyrimidine-5-carboxylate (**GLS4**). Yellow solid, yield 79%, mp: 124–127 °C; ¹H NMR (400 MHz, DMSO) δ 9.69 (s, 1H), 8.04 (d, *J* = 3.1 Hz, 1H), 7.95 (d, *J* = 2.5 Hz, 1H), 7.57 (dd, *J* = 8.5, 1.9 Hz, 1H), 7.40 (dd, *J* = 8.6, 6.2 Hz, 1H), 7.22 (td, *J* = 8.5, 2.4 Hz, 1H), 6.04 (s, 1H), 4.03–3.85 (m, 4H), 3.68 (t, *J* = 4.2 Hz, 4H), 2.55 (t, *J* = 7.2 Hz, 4H), 1.06 (t, *J* = 7.1 Hz, 3H); EI-MS: 509.4 [M+H]⁺.

General procedure for the synthesis of target compounds II-(1-10). To the mixture solution of intermediate **4** (0.20 g, 0.43 mmol) in THF (6 mL) and water (6 mL) were added with CuSO₄·5H₂O (0.01g, 0.043 mmol), Sodium ascorbate (0.025g, 0.13 mmol) and different acetylenes (0.86 mmol). The resulting mixture was stirred overnight at room temperature. Water (100 mL) was added to the residue and extrated with EtOAc (25 mL × 3), and the

organic phase was washed with saturated sodium chloride (25 mL), dried over anhydrous Na₂SO₄ and evaporated under reduced pressure to give the corresponding crude product. The residue was dissolved in a small amount EtOAc and purified by column chromatography on silica gel using PE-EA system to give **II-(1-10)** in good yield.

Ethyl

6-((4-(2-aminophenyl)-1H-1,2,3-triazol-1-yl)methyl)-4-(2-bromo-4-fluorophenyl)-2-(thiazol-2-yl)-1,4-dihydropyrimidine-5-carboxylate (**II-1**). Yellow solid, yield: 73%, mp: 184–187 °C; ¹H NMR (400 MHz, CDCl₃) δ: 8.08 (s, 1H), 7.79 (d, J = 3.1 Hz, 1H), 7.52 (s, 1H), 7.47 (d, J = 3.1 Hz, 1H), 7.43 (dd, J = 7.7, 1.3 Hz, 1H), 7.34 (ddd, J = 9.3, 8.4, 4.2 Hz, 2H), 7.16–7.07 (m, 1H), 7.03 (td, J = 8.3, 2.5 Hz, 1H), 6.77 (dd, J = 6.6, 5.9 Hz, 1H), 6.72 (dd, J = 11.6, 4.3 Hz, 1H), 6.17 (t, J = 15.1 Hz, 1H), 5.94 (dd, J = 39.1, 15.3 Hz, 2H), 5.54 (s, 2H), 4.14 (q, J = 7.2 Hz, 2H), 1.17 (t, J = 7.1 Hz, 3H); ¹³C NMR (100 MHz, CDCl₃): 165.02, 162.10 (d, J = 252.8 Hz), 161.77, 152.47, 150.09, 147.97, 145.20, 143.95, 137.62, 130.77 (d, J = 8.8 Hz), 128.78, 127.74, 125.06, 122.04 (d, J = 9.7 Hz), 121.84, 120.37 (d, J = 24.7 Hz), 117.24, 116.67, 115.85 (d, J = 21.1 Hz), 114.17, 106.48, 60.92, 52.12, 52.00, 14.08; EI-MS: 582.3 [M+H]⁺.

Ethyl

6-((4-(3-aminophenyl)-1H-1,2,3-triazol-1-yl)methyl)-4-(2-bromo-4-fluorophenyl)-2-(thiazol-2-yl)-1,4-dihydropyrimidine-5-carboxylate (**II-2**). Yellow solid, yield: 75%, mp: 148–151 °C; ¹H NMR (400 MHz, CDCl₃) δ: 8.02 (s, 1H), 7.78 (d, J = 3.1 Hz, 1H), 7.54 (s, 1H), 7.45 (d, J = 3.1 Hz, 1H), 7.41–7.28 (m, 3H), 7.23–7.15 (m, 2H), 7.03 (td, J = 8.3, 2.5 Hz, 1H), 6.73–6.58 (m, 1H), 6.17 (d, J = 32.5 Hz, 1H), 5.92 (q, J = 15.4 Hz, 2H), 4.13 (q, J = 7.1 Hz, 2H), 3.77 (s, 2H), 1.16 (t, J = 7.1 Hz, 3H); ¹³C NMR (100 MHz, CDCl₃): 165.04, 162.08 (d, J = 252.8 Hz), 161.82, 152.60, 150.06, 147.41, 146.88, 143.93, 137.66 (d, J = 3.4 Hz), 132.04, 130.80 (d, J = 8.8 Hz), 129.71, 125.07, 123.28, 122.03 (d, J = 9.7 Hz), 121.70, 120.34 (d, J = 24.7 Hz), 116.10, 115.82 (d, J = 21.1 Hz), 114.69, 112.34, 106.33, 60.90, 52.12, 52.00, 14.08; EI-MS: 582.3 [M+H]⁺.

Ethyl

4-(2-bromo-4-fluorophenyl)-6-((4-(pyridin-2-yl)-1*H*-1,2,3-triazol-1-yl)methyl)-2-(thiazol-2-yl)-1,4-dihydropyrimidine-5-carboxylate (**II-3**). Yellow solid, yield: 74%, mp: 194–197 °C; ¹H NMR (400 MHz, CDCl₃) δ: 8.59 (d, *J* = 4.8 Hz, 1H), 8.39 (s, 1H), 8.22 (d, *J* = 7.9 Hz, 1H), 7.84–7.71 (m, 2H), 7.53 (s, 1H), 7.43 (d, *J* = 3.1 Hz, 1H), 7.38 (dd, *J* = 8.6, 5.9 Hz, 1H), 7.32 (dd, *J* = 6.6, 4.0 Hz, 1H), 7.22 (ddd, *J* = 7.5, 4.9, 1.1 Hz, 1H), 7.04 (td, *J* = 8.3, 2.5 Hz, 1H), 6.13 (d, *J* = 2.4 Hz, 1H), 5.95 (dd, *J* = 31.5, 15.3 Hz, 2H), 4.14 (q, *J* = 7.1 Hz, 2H), 1.16 (t, *J* = 7.1 Hz, 3H); ¹³C NMR (100 MHz, CDCl₃): 164.97, 162.08 (d, *J* = 252.7 Hz), 161.83, 152.44, 150.77, 150.12, 149.41, 148.02, 143.87, 137.69 (d, *J* = 3.5 Hz), 136.81, 130.81 (d, *J* = 8.8 Hz), 125.04, 123.71, 122.61, 122.02 (d, *J* = 9.7 Hz), 120.45, 120.27, 120.20, 115.85 (d, *J* = 21.1 Hz), 106.58, 60.91, 52.31, 51.99, 14.07; EI-MS: 568.4 [M+H]⁺.

Ethyl

4-(2-bromo-4-fluorophenyl)-2-(thiazol-2-yl)-6-((4-(thiophen-2-yl)-1*H*-1,2,3-triazol-1-yl)methyl)-1,4-dihydropyrimidine-5-carboxylate (**II-4**). Yellow solid, yield: 76%, mp: 108–110 °C; ¹H NMR (400 MHz, CDCl₃) δ: 7.99 (s, 1H), 7.79 (d, *J* = 3.1 Hz, 1H), 7.52 (s, 1H), 7.47 (d, *J* = 3.1 Hz, 1H), 7.44–7.39 (m, 1H), 7.39–7.27 (m, 3H), 7.08 (dd, *J* = 5.0, 3.6 Hz, 1H), 7.04 (td, *J* = 8.3, 2.6 Hz, 1H), 6.13 (s, 1H), 5.91 (q, *J* = 15.5 Hz, 2H), 4.21–4.07 (m, 2H), 1.17 (t, *J* = 8.3 Hz, 3H); ¹³C NMR (100 MHz, CDCl₃): 165.01, 162.11 (d, *J* = 252.8 Hz), 161.77, 152.38, 150.07, 143.96, 142.38, 137.61 (d, *J* = 3.6 Hz), 133.53, 130.78 (d, *J* = 8.8 Hz), 127.64 (d, *J* = 10.3 Hz), 125.04, 124.72, 123.91, 122.04 (d, *J* = 9.7 Hz), 121.28, 120.37 (d, *J* = 24.6 Hz), 115.84 (d, *J* = 21.0 Hz), 106.41, 60.93, 52.14, 52.00, 14.07; EI-MS: 573.4 [M+H]⁺.

Ethyl

4-(2-bromo-4-fluorophenyl)-6-((4-phenyl-1*H*-1,2,3-triazol-1-yl)methyl)-2-(thiazol-2-yl)-1,4-dihydropyrimidine-5-carboxylate (**II-5**). Yellow solid, yield: 71%, mp: 109–112 °C; ¹H NMR (400 MHz, CDCl₃) δ: 8.07 (s, 1H), 7.90 (d, *J* = 1.3 Hz, 1H), 7.88 (s, 1H), 7.78 (d, *J* = 3.1 Hz, 1H), 7.54 (s, 1H), 7.48–7.29 (m, 6H), 7.03 (td, *J* = 8.3, 2.6 Hz, 1H), 6.13 (s, 1H), 5.93 (dd, *J* = 36.0, 15.4 Hz, 2H), 4.14 (q, *J* = 7.1 Hz, 2H), 1.17 (t, *J* = 7.1 Hz, 3H); ¹³C NMR (101 MHz, CDCl₃): 165.04, 162.09 (d, *J* = 252.8 Hz), 161.81, 152.55, 150.06, 147.33, 137.65 (d, *J* = 3.5

Hz), 131.14, 130.80 (d, J = 8.8 Hz), 128.91, 128.81, 127.89, 125.84, 125.75, 125.01, 122.05 (d, J = 9.7 Hz), 121.66, 120.36 (d, J = 24.6 Hz), 115.82 (d, J = 21.1 Hz), 106.41, 60.91, 52.13, 52.01, 14.08; EI-MS: 567.4 [M+H]⁺.

Ethyl

6-((4-(4-aminophenyl)-1H-1,2,3-triazol-1-yl)methyl)-4-(2-bromo-4-fluorophenyl)-2-(thiazol-2-yl)-1,4-dihydropyrimidine-5-carboxylate (**II-6**). Yellow solid, yield: 52%, mp: 123–127 °C; ¹H NMR (400 MHz, CDCl₃) δ: 7.93 (s, 1H), 7.78 (d, J = 3.0 Hz, 1H), 7.68 (d, J = 8.2 Hz, 2H), 7.52 (s, 1H), 7.45 (d, J = 2.8 Hz, 1H), 7.40–7.34 (m, 1H), 7.32 (dd, J = 8.1, 2.5 Hz, 1H), 7.02 (t, J = 9.1 Hz, 1H), 6.74 (d, J = 8.5 Hz, 2H), 6.17 (d, J = 29.7 Hz, 1H), 5.90 (q, J = 15.2 Hz, 2H), 4.13 (q, J = 7.1 Hz, 2H), 3.78 (s, 2H), 1.17 (t, J = 7.1 Hz, 3H); ¹³C NMR (100 MHz, CDCl₃): 165.05, 162.08 (d, J = 252.6 Hz), 161.88, 152.71, 150.04, 147.66 (s), 146.26, 143.91, 137.64, 130.81 (d, J = 8.9 Hz), 126.96, 125.01, 121.98, 121.74, 120.35, 120.33 (d, J = 24.6 Hz), 115.81 (d, J = 21.1 Hz), 115.27, 106.37, 60.89, 52.08, 51.99, 14.08; EI-MS: 582.3 [M+H]⁺.

Ethyl

6-((1H-1,2,3-triazol-1-yl)methyl)-4-(2-bromo-4-fluorophenyl)-2-(thiazol-2-yl)-1,4-dihydropyrimidine-5-carboxylate (**II-7**). Yellow solid, yield: 72%, mp: 115–119 °C; ¹H NMR (400 MHz, CDCl₃) δ: 7.85 (d, J = 0.7 Hz, 1H), 7.80 (d, J = 3.1 Hz, 1H), 7.75 (s, 1H), 7.52 (s, 1H), 7.49 (d, J = 3.1 Hz, 1H), 7.39–7.28 (m, 2H), 7.03 (td, J = 8.3, 2.6 Hz, 1H), 6.13 (d, J = 2.4 Hz, 1H), 5.95 (s, 1H), 5.90 (s, 1H), 4.13 (q, J = 7.1 Hz, 2H), 1.15 (t, J = 7.1 Hz, 3H); ¹³C NMR (100 MHz, CDCl₃): 165.00, 162.08 (d, J = 252.8 Hz), 161.81, 152.58, 150.03, 143.97, 137.64 (d, J = 3.5 Hz), 133.35, 130.76 (d, J = 8.8 Hz), 125.23, 124.90, 122.03 (d, J = 9.6 Hz), 120.34 (d, J = 24.6 Hz), 115.80 (d, J = 21.1 Hz), 106.44, 60.88, 51.96, 51.85, 14.05; EI-MS: 491.4 [M+H]⁺.

Ethyl

4-(2-bromo-4-fluorophenyl)-6-((4-(1-hydroxypentyl)-1H-1,2,3-triazol-1-yl)methyl)-2-(thiazol-2-yl)-1,4-dihydropyrimidine-5-carboxylate (**II-8**). Yellow solid, yield: 61%, mp: 79–83 °C;

¹H NMR (400 MHz, CDCl₃) δ: 7.78 (d, J = 3.1 Hz, 1H), 7.76 (s, 1H), 7.46 (d, J = 2.9 Hz, 1H), 7.39–7.25 (m, 2H), 7.02 (td, J = 8.3, 2.3 Hz, 1H), 6.13 (s, 1H), 5.93 (dd, J = 15.4, 7.7 Hz, 1H), 5.82 (dd, J = 15.4, 7.5 Hz, 1H), 4.93 (t, J = 6.5 Hz, 1H), 4.11 (q, J = 7.1 Hz, 2H), 2.60 (s, 1H), 1.99–1.84 (m, 2H), 1.63–1.28 (m, 4H), 1.15 (t, J = 7.1 Hz, 3H), 0.88 (t, J = 7.1 Hz, 3H); EI-MS: 577.5 [M+H]⁺.

Ethyl

4-(2-bromo-4-fluorophenyl)-6-((4-((4-methylbenzamido)methyl)-1H-1,2,3-triazol-1-yl)methyl)-2-(thiazol-2-yl)-1,4-dihydropyrimidine-5-carboxylate (**II-9**). Yellow solid, yield: 47%, mp: 85–89 °C; ¹H NMR (400 MHz, CDCl₃) δ: 7.93 (s, 1H), 7.72 (d, J = 8.1 Hz, 2H), 7.70 (d, J = 3.1 Hz, 1H), 7.30 (ddd, J = 15.0, 7.8, 5.2 Hz, 3H), 7.20 (d, J = 7.9 Hz, 2H), 7.15 (s, 1H), 7.00 (td, J = 8.3, 2.5 Hz, 1H), 6.11 (s, 1H), 5.89 (dd, J = 40.6, 15.7 Hz, 2H), 4.76 (d, J = 5.2 Hz, 2H), 4.11 (q, J = 7.1 Hz, 2H), 2.37 (s, 3H), 1.14 (t, J = 7.1 Hz, 3H); EI-MS: 638.3 [M+H]⁺.

Ethyl

4-(2-bromo-4-fluorophenyl)-2-(thiazol-2-yl)-6-((4-((2,4,6-trimethylphenylsulfonamido)methyl)-1H-1,2,3-triazol-1-yl)methyl)-1,4-dihydropyrimidine-5-carboxylate (**II-10**). Yellow solid, yield: 61%, mp: 96–99 °C; ¹H NMR (400 MHz, CDCl₃) δ: 7.81 (d, J = 3.1 Hz, 1H), 7.69 (s, 1H), 7.51 (d, J = 3.1 Hz, 2H), 7.36–7.29 (m, 2H), 7.04 (td, J = 8.3, 2.5 Hz, 1H), 6.95 (s, 2H), 6.12 (d, J = 2.5 Hz, 1H), 5.05 (t, J = 6.0 Hz, 1H), 4.25 (d, J = 6.1 Hz, 2H), 4.12 (d, J = 7.1 Hz, 3H), 2.65 (s, 6H), 2.31 (s, 3H), 1.15 (t, J = 7.1 Hz, 3H); ¹³C NMR (100 MHz, CDCl₃): 164.94, 162.09 (d, J = 252.9 Hz), 161.70, 152.26, 150.06, 144.00, 142.94, 142.34, 139.11, 137.63 (d, J = 3.5 Hz), 133.50, 132.01, 130.77 (d, J = 8.8 Hz), 125.08, 124.14, 122.02 (d, J = 9.7 Hz), 120.35 (d, J = 24.7 Hz), 115.85 (d, J = 21.1 Hz), 106.36, 60.89, 58.31, 51.97, 38.34, 22.98, 20.95, 14.05; EI-MS: 702.4 [M+H]⁺.

In Vitro Anti-HBV Assay.¹⁹ HepG2.2.15 cell lines are HBV-transfected hepatoma cell lines, which can stably secrete HBsAg, HBeAg, HBV DNA, HBV RNA, cccDNA and intact virus particles for a long time. It is the most widely used HBV drug screening cell model. HepG2.2.15 cell lines were obtained from the cell bank of the Chinese Academy of Sciences.

The cell lines were maintained in MEM medium supplemented with 10% fetal bovine serum, 100 U/mL penicillin, 100 µg/mL streptomycin, and 0.38 mg/mL of G418. Designed compounds were evaluated their in-vitro biological activities on the HepG2.2.15 cell line. After adding compounds, the HBV particles and antigens in the cell culture supernatant will change. Cytotoxicity was tested using CCK-8 method (CCK-8; Dojindo, Tokyo, Japan). Anti-HBV DNA replication activities were tested by real-time PCR assay. The anti-HBV antigen secretion activities were tested by enzyme linked immunosorbent assay (ELISA; Autobio Diagnostics Co., Ltd, China).

Toxicity measurements.²⁰ Cytotoxicity of tested compounds to HepG2.2.15 cells were assessed via CCK-8 method. Five different doses of tested compounds were added to 96-well tissue culture plates with 4000 cells in every well. Untreated cells with media alone were used as controls. The culture medium was replaced with a fresh one on day 4. After 8-day in triplicate of cell culture, 10% CCK-8 solution was added 0.5 h before the end of culture. OD absorbance values at 450 nm were collected by microplate reader (Bio-Rad, model 550) and the cell death percent was calculated.

Real time fluorescent PCR.¹⁸ HepG2.2.15 cells were cultured in triplicate of 96-well tissue culture plates with five different doses of tested compounds. The culture medium was replaced with a fresh one on day 4 during the 8-day experiment. Untreated cells with media alone were used as controls. On day 8, the supernatants of HepG2.2.15 cell were collected, which were quantified their HBV DNA using PCR-fluorescent probing (Quantitative diagnostic kit for HBV DNA). Briefly, 100 µL of the supernatants were added into the extraction buffer, boiled for 10 min and centrifuged for 10 min, and then proper aliquots were used for the fluorescent probing PCR. After PCR was run, the results were analyzed.

Inhibiting the secretion of HBeAg and HBsAg.²¹ HepG2.2.15 cells were cultured in triplicate of 96-well tissue culture plates with five different doses of tested compounds. The culture medium was replaced with a fresh one on day 4 during the 8-day experiment. Untreated cells with media alone were used as controls. On day 8, aspirate cell supernatant

and detect content of HBeAg and HBsAg by using diagnostic kit (Autobio Diagnostics Co., Ltd, China). The absorbance (A) of tested compounds were determined on microtiter plate ELISA reader. Drug inhibition ratio = (A normal cell group - A experimental group)/(A normal cell group - A blank group) \times 100%.

Molecular Docking. Molecular modeling was performed with the Tripos molecular modeling package Sybyl-X 2.0. All the molecules for docking were built using standard bond lengths and angles from Sybyl-X 2.0/Base Builder. The molecule (**II-1**) was optimized by using the Tripos force field for 1000 generations two times or more until the minimized conformers of the ligand were the same. The protein was prepared by removing the water molecules and ligand and adding polar hydrogen atoms. The published crystal structure of the liganded HBV capsid complex (PDB codes: 5e0i) was retrieved from the Protein Data Bank. The flexible docking method (Surflex-Dock) docks the ligand automatically into the ligand-binding site of the receptor by using a protocol-based approach and an empirically-derived scoring function. The protocol is a computational representation of a putative ligand that binds to the intended binding site and is a unique and essential element of the docking algorithm. The scoring function in Surflex-Dock, containing hydrophobic, polar, repulsive, entropic, and solvation terms, was trained to estimate the dissociation constant (K_d) expressed in $-\log(K_d)^2$. Surflex-Dock default settings were used for other parameters, such as the maximum number of rotatable bonds per molecule (set to 100) and the maximum number of poses per ligand (set to 20). During the docking procedure, all of the single bonds in residue side-chains inside the defined HBV capsid binding pocket were regarded as rotatable or flexible, and the ligand was allowed to rotate at all single bonds and move flexibly within the tentative binding pocket. The atomic charges were recalculated using the Kollman all-atom approach for the protein and the GasteigereHückel approach for the ligand. The binding interaction energy was calculated, including van der Waals, electrostatic, and torsional energy terms defined in the Tripos force field. The structure optimization was performed for 10,000 generations using a genetic algorithm, and the 20-best-scoring ligand-protein complexes were kept for further analysis. The $-\log(K_d)^2$ values of the 20-best-scoring complexes, representing the binding affinities of ligand with HBV capsid,

encompassed a wide range of functional classes (10^{-2} - 10^{-9}). Hence, only the highest-scoring 3D structural model of ligand-bound HBV capsid was chosen to define the binding interaction.

Funding

Financial support from the National Natural Science Foundation of China (NSFC Nos. 81273354, 81573347), Key Project of NSFC for International Cooperation (No. 81420108027), Young Scholars Program of Shandong University (YSPSDU, No. 2016WLJH32), the Fundamental Research Funds of Shandong University (No. 2017JC006), Key research and development project of Shandong Province (No. 2017CXGC1401), Key Laboratory of Chemical Biology (Ministry of Education) Open Projects Fund (No. CB-201715) and Major Project of Science and Technology of Shandong Province (No. 2015ZDJS04001) is gratefully acknowledged.

Notes

The authors declare no competing financial interest.

ABBREVIATIONS

HAPs, heteroaryldihydropyrimidines; SARs, structure-activity relationships; CHB, Chronic hepatitis B; HBV, hepatitis B virus; HCC, hepatocellular carcinoma; NRTIs, nucleoside/nucleotide reverse transcriptase inhibitors; 3TC, lamivudine; ETV, entecavir; LdT, telbivudine; ADV, adefovir dipivoxil; TDF, tenofovir disoproxil; TAF, tenofovir alafenamide; cccDNA, covalently closed circular DNA; pgRNA, pregenomic RNA; FDA, Food and Drug Administration; IC₅₀, the concentration causing 50% inhibition of antiviral activity; CC₅₀, 50% cytotoxicity concentration; SI, selection index.

FIGURE LEGENDS

Figure 1. The structures of six NRTIs approved by US FDA for HBV therapy.

Figure 2. The structures of four HBV capsid inhibitors.

Figure 3. 4-methyl HAPs (green, PDB ID: 5GMZ) and sulfamoylbenzamides (yellow, PDB ID: 5T2P) bind in Hepatitis B virus core protein Y132A mutant. The result was displayed by PyMOL.

Figure 4. The design of target compounds.

Figure 5. (a) Predicted binding mode of compound **II-1** in HBV capsid (PDB ID: 5e0i); (b) Surface presentation of **II-1** located toward a solvent exposure region. Hydrogen bonds are indicated with dashed lines in red, and all the non-polar hydrogen atoms are omitted for clarity.

REFERENCES

- (1) Schinazi, R. F.; Ehteshami, M.; Bassit, L.; Asselah, T. Towards HBV curative therapies. *Liver International*. **2018**, 38, 102–114.
- (2) Lin, C.; Yang, H.; Kao, J. Hepatitis B virus: new therapeutic perspectives. *Liver International: Official Journal of the International Association for the Study of the Liver*. **2016**, 36, 85–92.
- (3) Tajiri, K.; Shimizu, Y. New horizon for radical cure of chronic hepatitis B virus infection. *World Journal of Hepatology*. **2016**, 8, 863–873.
- (4) De Clercq, E. Current treatment of hepatitis B virus infections. *Reviews in Medical Virology*. **2015**, 25, 354–365.
- (5) Liaw, Y.; Chu, C. Hepatitis B virus infection. *Seminars in Fetal & Neonatal Medicine*. **2009**, 373, 582–592.
- (6) Liu, N.; Zhao, F.; Zhan, P.; Liu, X. Review of Small Synthetic Molecules Targeting HBV Capsid Assembly. *Medicinal Chemistry*. **2015**, 11, 710–716.

(7) Bourne, C.; Lee, S.; Venkataiah, B.; Lee, A.; Korba, B.; Finn, M. G.; Zlotnick, A. Small-Molecule Effectors of Hepatitis B Virus Capsid Assembly Give Insight into Virus Life Cycle. *Journal of Virology*. **2008**, 82, 10262–10270.

(8) Grimm, D.; Thimme, R.; Blum, H. HBV life cycle and novel drug targets. *Hepatology International*. **2011**, 5, 644–653.

(9) Qiu, Z.; Lin, X.; Zhang, W.; Zhou, M.; Guo, L.; Kocer, B.; Wu, G.; Zhang, Z.; Liu, H.; Shi, H.; Kou, B.; Hu, T.; Hu, Y.; Huang, M.; Yan, S.; Xu, Z.; Zhou, Z.; Qin, N.; Wang, Y.; Ren, S.; Qiu, H.; Zhang, Y.; Zhang, Y.; Wu, X.; Sun, K.; Zhong, S.; Xie, J.; Ottaviani, G.; Zhou, Y.; Zhu, L.; Tian, X.; Shi, L.; Ren, F.; Mao, Y.; Zhou, X.; Gao, L.; Young, J.; Wu, J.; Yang, G.; Mayweg, A.; Shen, H.; Tang, G.; Zhu, W. Discovery and Pre-Clinical Characterization of a 3(rd) Generation 4-H HeteroAryldihydroPyrimidine (HAP) Analogues as Hepatitis B Virus (HBV) Capsid Inhibitors. *Journal of Medicinal Chemistry*. **2017**, 60, 3352–3371.

(10) Wu, G.; Liu, B.; Zhang, Y.; Li, J.; Arzumanyan, A.; Clayton, M. M.; Schinazi, R. F.; Wang, Z.; Goldmann, S.; Ren, Q.; Zhang, F.; Feitelson, M. A. Preclinical characterization of GLS4, an inhibitor of hepatitis B virus core particle assembly. *Antimicrobial Agents & Chemotherapy*. **2013**, 57, 5344–5354.

(11) Zhou, X.; Li, L.; Deng, P.; Chen, X.; Zhong, D. Characterization of metabolites of GLS4 in humans using ultrahigh-performance liquid chromatography/quadrupole time-of-flight mass spectrometry. *Rapid Communications in Mass Spectrometry: Rcm*. **2013**, 27, 2483–2492.

(12) Qiu, Z.; Lin, X.; Zhou, M.; Liu, Y.; Zhu, W.; Chen, W.; Zhang, W.; Guo, L.; Liu, H.; Wu, G.; Huang, M.; Jiang, M.; Xu, Z.; Zhou, Z.; Qin, N.; Ren, S.; Qiu, H.; Zhong, S.; Zhang, Y.; Zhang, Y.; Wu, X.; Shi, L.; Ren, F.; Mao, Y.; Zhou, X.; Yang, W.; Wu, J.; Yang, G.; Mayweg, A.; Shen, H.; Tang, G. Design and Synthesis of Orally Bioavailable 4-Methyl Heteroaryldihydropyrimidine Based Hepatitis B Virus (HBV) Capsid Inhibitors. *Journal of Medicinal Chemistry*. **2016**, 59, 7651–7666.

(13) Li, X.; Zhou, K.; He, H.; Zhou, Q.; Sun, Y.; Hou, L.; Shen, L.; Wang, X.; Zhou, Y.; Gong, Z.; He, S.; Jin, H.; Gu, Z.; Zhao, S.; Zhang, L.; Sun, C.; Zheng, S.; Cheng, Z.; Zhu, Y.; Zhang, M.; Li, J.; Chen, S. Design, Synthesis, and Evaluation of

Tetrahydropyrrolo[1,2-c]pyrimidines as Capsid Assembly Inhibitors for HBV Treatment. *Acs Medicinal Chemistry Letters*. **2017**, 8, 969–974.

(14) Abbate, F.; Supuran, C. T.; Scozzafava, A.; Orioli, P.; Stubbs, M. T.; Klebe, G. Nonaromatic sulfonamide group as an ideal anchor for potent human carbonic anhydrase inhibitors: role of hydrogen-bonding networks in ligand binding and drug design. *Journal of Medicinal Chemistry*. **2002**, 45, 3583–3587.

(15) Modak, J. K.; Liu, Y.; Supuran, C. T.; Roujeinikova, A. Structure-Activity Relationship for Sulfonamide Inhibition of Helicobacter pylori α -Carbonic Anhydrase. *Journal of Medicinal Chemistry*. **2016**, 59, 11098–11109.

(16) He, H.; Zhou, K.; Qin, H.; Zhou, Y.; Wang, X.; Chi, X.; Li, J.; Chen, S. Dihydropyrimido loop dertvative as HBV inhibitor. *Faming Zhuanli Shenqing*. **2015**, WO2015180631A1.

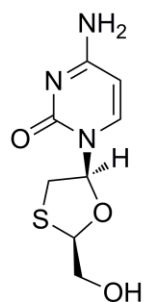
(17) Williams, J. D.; Khan, A. R.; Cardinale, S. C.; Butler, M. M.; Bowlin, T. L.; Peet, N. P. Small molecule inhibitors of anthrax lethal factor toxin. *Bioorganic & Medicinal Chemistry*. **2014**, 22, 419–434.

(18) Jia, H.; Bai, F.; Liu, N.; Liang, X.; Ma, C.; Jiang, X.; Liu, X. Design, synthesis and evaluation of pyrazole derivatives as non-nucleoside hepatitis B virus inhibitors. *European Journal of Medicinal Chemistry*. **2016**, 123, 202–210.

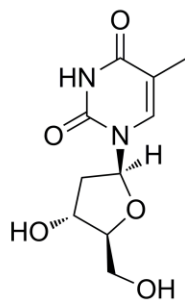
(19) Jia, H.; Rai, D.; Zhan, P.; Chen, X.; Jiang, X.; Liu, X. Recent advance of the hepatitis B virus inhibitors: a medicinal chemistry overview. *Future Medicinal Chemistry*. **2015**, 7, 587–607.

(20) Li, Z.; Luo, W.; Fu, Y.; Jiang, Q.; Liu, J.; Wu, Z. Inhibition of HBV replication by constructing an artificial transcription factor. *Chinese Journal of Cellular & Molecular Immunology*. **2015**, 31, 1322–1326.

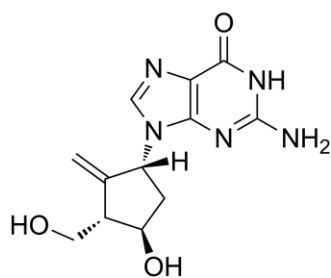
(21) Jia, H.; Song, Y.; Yu, J.; Zhan, P.; Rai, D.; Liang, X.; Ma, C.; Liu, X. Design, synthesis and primary biological evaluation of the novel 2-pyridone derivatives as potent non-nucleoside HBV inhibitors. *European Journal of Medicinal Chemistry*. **2017**, 136, 144–153.



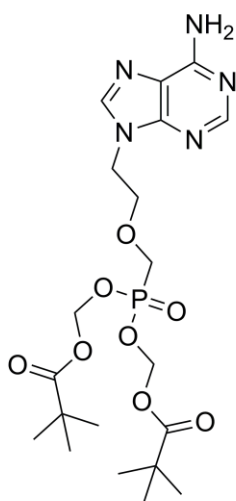
Lamivudine



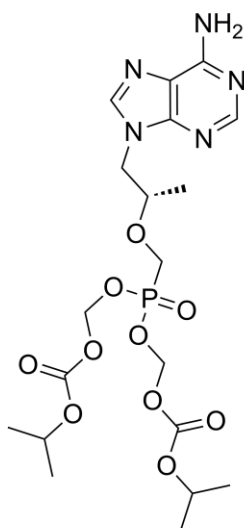
Telbivudine



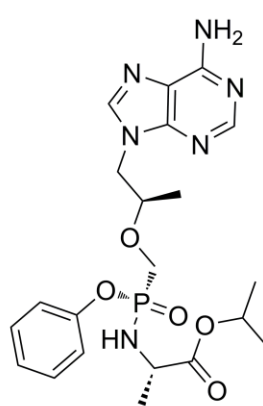
Entecavir



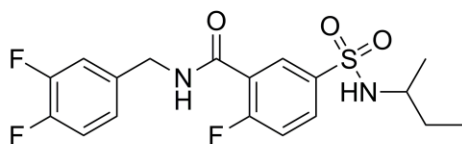
Adefovir dipivixil



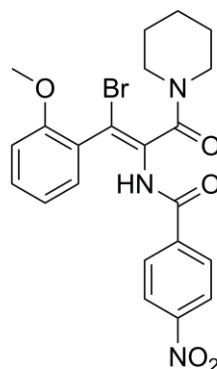
Tenofovir disoproxil



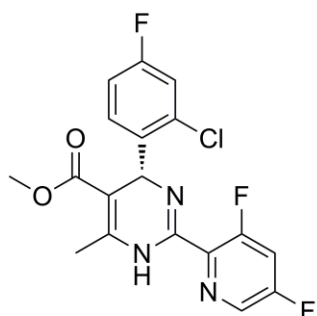
Tenofovir alafenamide

**DVR-23**

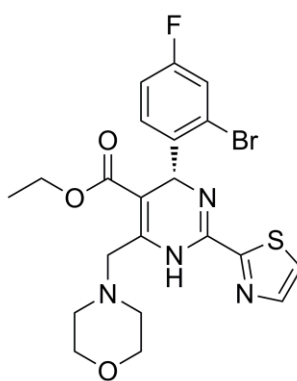
HepDES19 cells, $IC_{50} = 0.1 \mu M$
 $CC_{50} > 50 \mu M$

**AT-130**

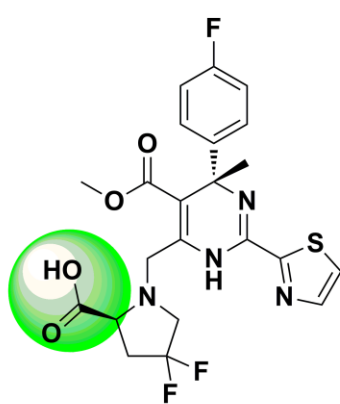
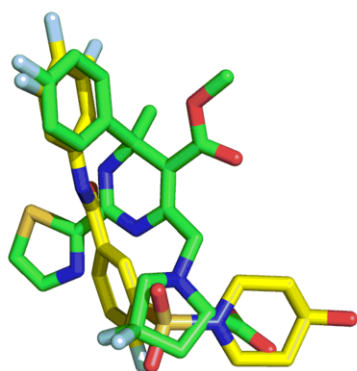
HepG2 cells, $IC_{50} = 2.4 \mu M$

**Bay 41-4109**

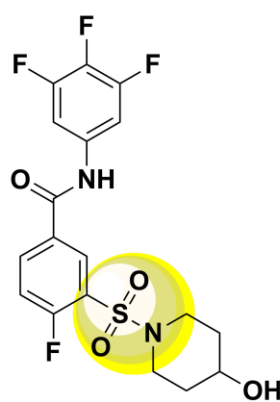
In HepAD38 cells, $IC_{50} = 124.25 \text{ nM}$
primary human hepatocytes, $CC_{50} = 35 \mu M$

**GLS4**

HepAD38 cells, $IC_{50} = 62.24 \text{ nM}$
adefovir-resistant strains, $IC_{50} = 12 \text{ nM}$
primary human hepatocytes, $CC_{50} = 115 \mu M$



4-methyl heteroaryldihydropyrimidine
2016, J.Med.Chem. $EC_{50} = 84$ nM



sulfamoylbenzamide (SBA-R01)

